Journal of Science and Technology Research

Journal homepage: www.nipesjournals.org.ng

Local-Global Description of Digital Images for Detection and Analysis of Medical Features

[1]Adekunle M. Ibrahim, [2]Funsho Abdulwahab
[1]Department of ICT, Osun State University, Osogbo, Nigeria
[2]Department of Computer Science, Universiti Utara Malaysia, Malaysia
*Corresponding Author Email: kunle_ibrahim2001@yahoo.com

Article Info

Abstract

This paper presents two descriptors to tackle the existing problems in medical imaging by providing more information to describe different textural structures of digital images. The proposed global and local descriptors can provide more accurate analysis of medical features by using hybrid concatenation approach. Several mathematical models in the form of local and global descriptors have been developed and used in the computation and analysis of medical problems. The experimental results showed that both local and global features are very useful in detection and analysis of biomedical features. The results also indicate that the global descriptor outperforms the earlier approaches and demonstrates high discriminating power and robustness of combined features for accurate classification of CT images.

1. Introduction

Ordinary human may find it difficult to visualize and extract general information from images or objects. The useful information extracted from those images or objects are referred to as features. These objects can be represented in form of two or three dimensions and the extracted features or useful information would be smaller in size compared to the original image. The reason for the size or dimensional reduction in the feature extracted is simply because some irrelevant materials must have been eliminated from the original images after applying preprocessing algorithms. This is a very important stage in image processing as the process would help programmers to focus on the important features that would greatly improve the computational accuracy of the experimental results. This process shows how important feature extraction is in image analysis. However, one must be very careful at this stage to ensure the important information is not being removed during this process. Some factors must be taken into consideration before you remove regions or parts of the image. In computing, we can develop an algorithm or construct a model to achieve favourable results in this process.

Local features can be different from global features since the former represents a subset of the latter. In other words, those features extracted from certain parts of the image or objects are local while global features capture the entire object. During the classification process, several patches or local

features can be extracted from a global image because global representation or descriptors describe the general property of the entire image. A very good example could be a multifractal model for effective analysis and classification of medical images developed by [1-6]. Multifractal descriptor represents a global description of images as it showcases the characteristic properties of the entire object while local features can be obtained from local binary patterns (LBP). Both descriptors could be used for medical image descriptions and analyses. Hopefully, a combination of the features from local and global descriptors could yield powerful features for efficient classification and analysis of images.

1.1. Techniques in Feature Extraction

Strong background knowledge in mathematics can help to manipulate image pixels and develop feature techniques that could be used to differentiate between two closely related objects. The techniques for feature extraction involve processing of intensity pixels by developing classification models for further analysis in images. Digital images with discrete pixels could be processed and manipulated to obtain discriminating features for efficient classification, detection, or identification of patterns of interest. Programmers and analysts can decide on how the information extracted from this object is processed by constructing models that could be used to measure the similarities and differences in image features. The developed models would transform all intensity pixels into meaningful information to expose all characteristic features for further processing. It depends on what you are trying to achieve, and how you intend to achieve them would also depend on the specification of the developed system and methods for gathering information during this process.

1.2. Computation of Local Features

The Higuchi's method is another efficient way of calculating the fractal dimension of a curve that has found several applications in the analysis of time series [7]. Higuchi's method is particularly suitable for a one-dimensional signal whose values at regular discrete intervals are available in the form $x(i)$, $i = 1, 2, ...N$. Several new data point series can be constructed using an interval length, and starting value index t:

$$S_t(\varphi) = \{x(t), x(t + \varphi), x(t + 2\varphi), \ldots \ldots x(t + p\varphi)\} \tag{1}$$

Where

$$p = [\frac{t-1}{\varphi}] \tag{2}$$

The length of the series in (4) is calculated as a normalized sum of differences:

$$l_r(\varphi) = \frac{N-1}{P\varphi^2}\sum_{i1}^{p} I \, x(t + i\varphi) - \, x(t + (i - 1)\varphi) \tag{3}$$

The mean length for each interval length is obtained as

$$L(\varphi) = \frac{1}{\varphi}\sum_{\varphi}^{1} L_k(\varphi) \tag{4}$$

As in the case of the box-counting dimension, the Higuchi dimension D_H is also computed as the slope of a linear regression line obtained using a log-log plot with log(φ) along the x-axis, and log (L(φ)) along the y-axis.

An *MxM* image *I(x, y)* must be converted to one-dimensional data before the above method can be applied. A common approach used for this is to add the values along each column to get a one-dimensional array of sums of pixel intensities:

$$x(x) = \sum_{y=1}^{M} I(x, y), j = 1, 2, \dots M. \tag{5}$$

1.3. Generalized Renyi Dimension

The Higuchi's dimension outlined above can be extended to a generalized family of dimensions called Renyi dimensions. These dimensions use a probability measure function μ. In the context of the box- counting algorithm, μ_i represents the probability of finding a point of fractal within a box with index *i*. The Renyi dimensions D_q are defined with respect to a non-negative parameter *q* as

$$D_q = \frac{1}{q-1} \lim_{\delta \to 0} \frac{log_2[\sum_{i=1}^{N} \mu_i^q]}{log_2 \delta} \tag{6}$$

As a special case of the above, when q becomes 0, we get the box counting dimension. In a fractal system the measured object is assumed to have an internal structure with different spatial scales; the number N(e) of features of certain size e scale as [8, 9].

1.4 Exact and Statistical Self-Similarity
The most important geometrical characteristic exhibited by fractals is self- similarity, which is the property of invariance under certain scale transformations. A fractal on a plane can be viewed as a bounded set *S* of two-dimensional points. The set *S* is self-similar if it is the union of *N* non-overlapping subsets, each of which is congruent to scaled versions of [12]. Two sets of points are congruent if by using a similarity transformation consisting of scaling, rotations, transformations and reflections; one set can be transformed into an exact copy of the other.

All real-world examples modelled using random fractals have statistical self-similarity. Here, different parts of a fractal cannot be made exactly congruent to the whole set even after an arbitrary rotational transformation and displacement. In this context, statistical self-similarity refers to the fact that enlargements of small constituent segments of a fractal have the same statistical distribution as the whole set [13]. In other words, parts of a random fractal can be matched with the whole set only in a statistical sense. In a broader context, statistical self-similarity refers to the characteristic of having a nearly constant measurement (within an allowable threshold) of certain statistical parameters derived from sets at various scales.

Several methods of multi-fractal analysis of medical images have been suggested and evaluated in different ways [14-20]. [14] developed a two-pass algorithm for the computation of multi-fractal spectrum and used the calculated spectra for the classification in a tissue image database. In [5], the holder exponent for the power law approximation of intensity measures in pixel neighbourhoods has been used for resolving local density variations in the CT lung images. This paper provides a processing pipeline for describing digital images in detection and analysis of region of interest in medical features.

2. Methodology

In this section, we give an overview of the computational stages in the analysis of images. The purpose of this section is to give an integrated view of the whole pipeline, showing the sequence of processes that should be implemented. In Figure 1, we provide a diagram of this processing pipeline consisting of three layers: the input layer, the computational layer and the output layer. Note that the output layer involves two types of α-histograms. The first α-histogram can be obtained directly from the α-image, where each α value is transformed into the range [0-255] and represented as a gray-level. The second α-histogram can be generated by discretizing the α -range [α_{min}, α_{max}] into *n* number of subintervals, and counting the number of pixels having α values in each subinterval. In order to evaluate the discriminating capability of the combined features from the two descriptors as demonstrated in Figure 1, different classification experiments have been investigated. Three Emphysema classes are defined with 50 images, assigned to each class. We employed two different image classifiers due to the nature of the datasets used in this study; the SVM, and random forests (RF) [21-24]. The RF could be a perfect classifier for the medical datasets since it is relatively robust to outliers and noise, and always enhance better accuracy when random features are used. The RF randomly selects inputs or a combination of inputs to grow each tree. This can significantly improve the classification accuracy by combining trees grown using random features, and the generalization error of the forests reduces as the number of trees becomes large [21].
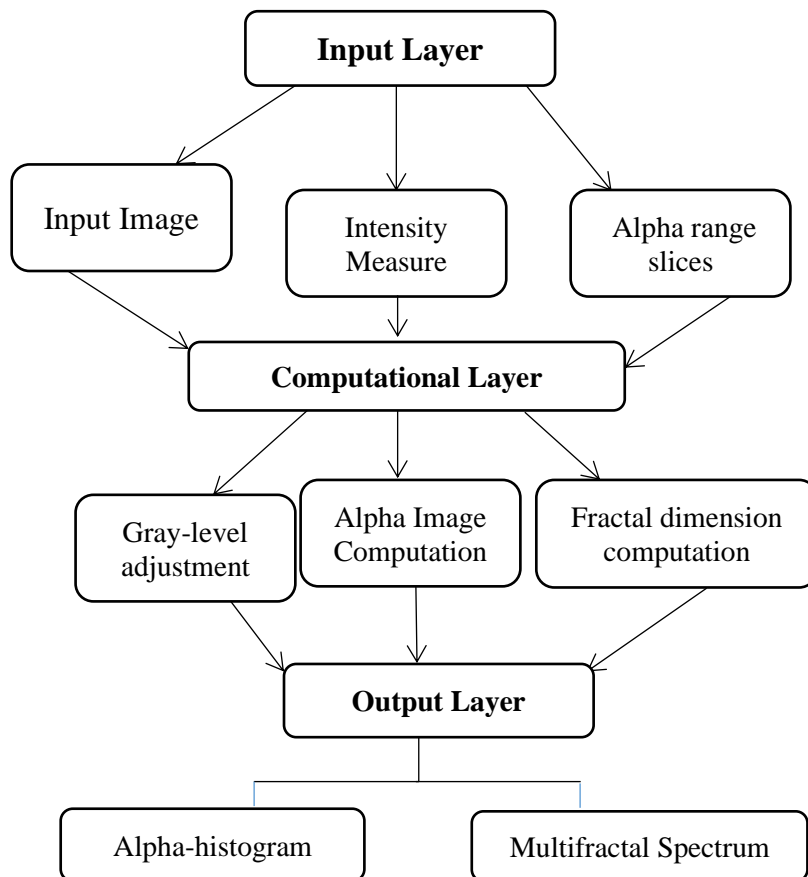
Figure 1: Main steps in the computation of multi-fractal spectrum of an input image.

3. Results and Discussion

SVMs have demonstrated highly competitive performance in many real-world applications, such as bioinformatics, face recognition and image processing. The results indicate that the global feature presents good classification performance, particularly with the RF classifier, though; the results obtained from the SVM are also good for the global features. As can be seen in Figure 1, it is noted from the results that the effects of the window size on the data sets are very obvious (Table 1).

Table 1: Classification Results of Global Descriptor

Classification accuracy – Global Feature		
Image Sizes	*SVM*	*Random Forest*
64 * 64	50.04%	73.17%
128 * 128	52.08%	81.52%
256 * 256	62.53%	92.45%
320 * 320	61.16%	94.38%
384 * 384	62.23%	96.13
512 * 512	61.51%	98.23%

In other words, the data sets with the largest image sizes gave the best classification accuracy, using two different classifiers while the data sets with the smallest image pixel size gave the lowest performance. These results also demonstrate that as the image size is increasing the overall classification accuracy is also increasing, which indicates that the larger the window size, the higher the classification accuracy. This is simply because the images with larger sizes have captured more useful information and feature, which eventually increases the discriminating power of the features used in the classification process. The original size of the image pattern does not contain enough discriminative information, which can lead to a reduction in the performance accuracy of the classification system. Overall, the performance of the global descriptor looks very good as the classification accuracy falls within the range of 73.17-98.23%. Generally, the RF classifier performed better than the SVM in all cases, since the classification accuracy of the SVM classifier falls within the range of 50.04–61.51%. The classification results of the local descriptor using different image sizes with two different image classifiers are presented in Table 2.

Table 2: Classification Results of Local Descriptor

Classification accuracy – Local Descriptor		
Image Sizes	*SVM*	*Random Forest*
64 * 64	47.34%	56.78%
128 * 128	48.25%	47.67%
256 * 256	49.89%	46.11%

Performances of the local descriptor are generally lower than that of the global descriptor. Similarly, the scale invariance of different image sizes does not have any significant impact on classification accuracy. However, in the global descriptor, the effect of image sizes of the patches is very obvious, this is expected because the data from the local descriptor do not really require further invariance examination as this has been done during implementation. It has been verified experimentally that the execution run time to generate global features is about 5 times faster than that of local features using the same image size. Take for instance, for a 128*128 pixel size, the local image run time was around 4.5s whereas it took just 0.9s to generate the global image of the same image size. Similarly, for a 512 * 512, the execution run time for the local image was around 46.74s while global images can be calculated in just 8.7s. The experimental tests for the time complexities were carried out for four different image sizes; that is; 64*64, 128*128, 256*256 and 512*512 for comparison between local and global image features. Generally, the local images consume more computational time than the global image (Table 3). The details of the computational time for both feature descriptors are

presented in Table 3 using different image patches. The framework of this study provided solutions to a few research questions in the field of image classifications. For instance, how does the feature extracted from local and global descriptors behave under the same scale changes? How does the descriptor generally compare with the previous work using other textural classification approaches? It has been demonstrated in this research work the effectiveness of global descriptors in the classification of medical images. In the experimental analysis, we could see how powerful this descriptor is and how it behaves under different scale changes.

This explains the importance of global features compared to the local features in detection of medical problems as the former behaves well under different image sizes. The second stage of the experiment compares the results obtained with the state-of-art method in recent article [16]. In Table 1, our results compare favourably with the LBP results [16], the overall classification accuracy of 98.23% from the global features with the RF classifier demonstrated that this descriptor performed better than the accuracy of 95.2% achieved by [16] for the classification of emphysema patterns. This shows that the features from the global descriptor have higher discriminative power than that of LBP.

Table 3: Computational Time Comparison Between Global Image and Local Image

Computational Time in seconds		
Image size	*Global image*	*Local Image*
64 *64	0.2957s	1.4531s
128 *128	0.9113s	4.5104s
256 * 256	2.3865s	11.15s
512 * 512	8.7017s	46.74s

4. Conclusion

In this study, global and local descriptors have been developed to extract the textural characteristics of digital images using some of the machine learning tools to identify regions or sections of medical patterns with severe problems. We have also demonstrated using the global descriptors that the window sizes of the image have great influence on the classification accuracy. We have analyzed the effect of different image sizes using two different descriptors. We have shown that the proposed descriptors could perform well even with big data sets, especially the global descriptor that has really shown excellent performances in all cases. This is a great achievement as the classification of large data sets involved in this experiment may sometimes pose some challenges that may affect the performances of the classification model. The combined feature that uses the global descriptor is better than the other descriptor (local) in terms of computational time and overall efficiency of data analysis.

References

[1] Ibrahim, M., & Mukundan, R. (2014). Multifractal Techniques for Emphysema Classification in Lung Tissue Images. *International Proceedings of Chemical,Biological & Environmental Engineering*, *78*, 115–119. Retrieved from http://www.etlibrary.org/?m=fbook&a=details&aid=15734

[2] Ibrahim, M., & Mukundan, R. (2015). Cascaded techniques for improving emphysema classification in computed tomography images. *Artificial Intelligence Research*, *4*(2), 112–118. doi:10.5430/air.v4n2p112

[3] Ibrahim M.A., Ojo O.A., Oluwafisoye P.A. (2017). On Feature Selection Methods for Accurate Classification and Analysis of Emphysema CT Images. *International Journal of Medical Imaging*, *SciencePG* 5(6), 2017,70-78.

[4] Ibrahim M.A., Ojo O.A., Oluwafisoye P.A. (2017). Analysis of Emphysema Patterns Computed Tomography Image, *International Journal of Scientific & Engineering Research,* 8(12), 2157-2168. https://www.ijser.org/research-paper-publishing-december- 2017_page6.aspx

[5] Ibrahim M.A., Ojo O.A, P.A. Oluwafisoye P.A. (2018). Identification of Emphysema Patterns in High Resolution Computed Tomography Images. *Journal of Biomedical Engineering and Informatics* (Canada, 2017), Sciedupress 4(1),16-24.

[6] Ibrahim M.A., Ojo O.A. "New Multi-fractal Techniques for Pattern Analysis in Biomedical Images", *SIA OmniSciptum Publishing, Latvia(2018), European Union;LAMBERT Academic Publishing: ISBN:978613989296-9.* https://www.omniscriptum.com

[7] Higuchi, T. (1988). North-Holland Physics Publishing Division. *Physical D 3l*, 277–283.\

[8] Miranda, J. G. V, Montero, E., Alves, M. C., González, A. P., & Vázquez, E. V. (2006). Multifractal characterization of saprolite particle-size distributions after topsoil removal. *Elsevier*, *l34*, 373–385. doi:10.1016/j.geoderma.2006.03.014

[9] Posadas, A. N. D., Giménez, D., Quiroz, R., & Protz, R. (2003). Multifractal Characterization of Soil Pore Systems. *Journal of Food Engineering*, *67*, 1–14.

[10] Chhabra, A., & Jensen, R. V. (1989). Physical Review letters. *Direct Determination of the F(alpha) Singularity Spectrum*, *62*(March), 1327– 1330.

[11] Oiwa, N., & Fiedler-Ferrara, N. (1998). Physical D. *Elsevier*, *l24*, 210– 224. Oudjemia, S., Girault, J., Derguini, N., & Haddab, S. (2013). Multifractal Analysis: Application to Medical Imaging., 244–249.

[12] Mandelbrot, B. B. (1977). *The Fractal Geometry of Nature*. New York: Martinez, F. S. J., Martin, M. A., Caniego, F. J., Tuller, M., Guber, A., & Pachepsky, Y. (1999). Multi fractal analysis of discretized X-ray CT images for the characterization of soil macropore structures.*Geoderma, l56*(2), 32-42.

[13] Falconer, K. (2003). Fractal Geometry- Mathematical Foundations and Applications. (2nd ed.). London: Wiley

[14] Hemsley, A., & Mukundan, R. (2009). Multifractal Measures for Tissue Image Classification and Retrieval. *llth IEEE International Symposium on Multimedia*, 618–623. doi:10.1109/ISM.2009.94\

[15] Nilsson, E. (2007). Multifractal-based Image Analysis with applications in Medical Imaging. Department of Computer Science, Umea University, Umea Sweden.

[16] Sørensen, L., Shaker, S. B., & Bruijne, M. De. (2010). Quantitative Analysis of Pulmonary Emphysema using Local Binary Patterns. *IEEE Transactions on Medical Imaging*, *29*(2), 559–569. doi:10.1109/TMI.2009.2038575

[17] Stojis, T., Reljin, I., & Reljin, B. (2006). Adaptation of multifractal analysis to segmentation of microcalcifications in digital mammograms. *Physica A: Statistical Mechanics and Its Applications*, *367*, 494–508. doi:S0378437105012331

[18] Stosis, T., & Stosis, B. D. (2006). Multifractal Analysis of Human Retinal Vessels. *IEEE Transactions on Medical Imaging*, *25*(8), 1101–1107.

[19] Thomazini, D., Gelfuso, M. V, & Altafim, R. A. C. (2008). Analysis of entropy and fractal dimension to classify the hydrophobicity in polymeric insulators. *Electrical Insulating Materials, 2OO8. (ISEIM 2OO8). International Symposium on*, (2), 279–282.doi:10.1109/ISEIM.2008.4664551

[20] Vasiljevic, J., Reljin, B., Sopta, J., Mijucic, V., Tulic, G., & Reljin, I. (2012). Application of multifractal analysis on microscopic images in the classification of metastatic bone disease. *Biomedical Microdevices*, *l4*, 541–548. doi:22327812

[21] Breiman, L. (2001). Random forests. *Machine Learning*, *45*, 5–32. doi:10.1023/A:1010933404324

[22] [Zaia, A., Eleonori, R., Maponi, P., Rossi, R., & Murri, R. (2006). MR imaging and osteoporosis: Fractal lacunarity analysis of trabecular bone. *IEEE Transactions on Information Technology in Biomedicine*, *lO*(3), 484–489. doi:10.1109/TITB.2006.872078

[23] Zhang, L., Member, S., Wang, L., Member, S., & Lin, W. (2012). Information for Collaborative Image Retrieval. *IEEE Transactions on Image Processing*, *2l*(8), 3707–3720.

[24] Appleby, S. (1996). Pattern of the Human Population. *Geographical Anaysis*, *28*(2), 147–160.